$Co[V_2]O_4$: A Spinel Approaching the Itinerant Electron Limit

A. Kismarahardja,[1,2] J. S. Brooks,[1,2] A. Kiswandhi,[1,2] K. Matsubayashi,[3] R. Yamanaka,[3] Y. Uwatoko,[3] J. Whalen,[1] T. Siegrist,[1,4] and H. D. Zhou[1,*]

[1]National High Magnetic Field Laboratory, Florida State University, Tallahassee, Florida 32306-4005, USA
[2]Department of Physics, Florida State University, Tallahassee, Florida 32306-3016, USA
[3]The Institute for Solid State Physics, The University of Tokyo, Kashiwa, Chiba 277-8581, Japan
[4]Department of Chemical and Biomedical Engineering, Florida State University, Tallahassee, Florida 32310, USA

(Received 29 July 2010; published 4 February 2011)

Studies of the structure, magnetization, and resistivity under pressure on stoichiometric normal spinel $Co[V_2]O_4$ single crystals show (i) absence of a structural distortion, (ii) abnormal magnetic critical exponents, and (iii) metallic conductivity induced by pressures at low temperatures. All these results prove that $Co[V_2]O_4$ sits on the edge of the itinerant-electron limit. Compared with similar measurements on $Fe[V_2]O_4$ and other $A[V_2]O_4$ studies, it is shown that a critical V-V separation for a localized-itinerant electronic phase transition exists.

DOI: 10.1103/PhysRevLett.106.056602 PACS numbers: 72.80.Ga, 71.30.+h, 75.30.Et, 75.50.Dd

Normal spinels $A[V_2]O_4$ ($A =$ Cd, Mn, Fe, Mg, Zn, and Co) has been a hot topic due to their complicated physical properties related to the strong spin-lattice coupling from the localized V^{3+} ($3d^2$) electrons with t_{2g} orbital freedom, and also their highly geometrically frustrated pyrochlore structure formed by corner-sharing tetrahedra on the V sites [1]. Another interesting aspect of $A[V_2]O_4$ is that the system approaches the itinerant-electron limit with decreasing V-V separation ($R_{\text{v-v}}$) [2,3]. The predicted critical separation for the metallic behavior is $R_c = 2.94$ Å [4]. In general, the spin-spin interaction for a magnetic insulator can be described as $J \propto t^2/U$, where t is the spin-dependent expectation value for the charge transfer between sites and U is the intra-atomic Coulomb energy [5]; t is also a function of the interionic distance, R. The Bloch's law $\alpha_B \equiv (d\ln T_N/dP)/(d\ln V/dP) \approx -3.3$ successfully describes this volume dependence, provided U remains constant [6]. However, pressure studies on magnetization of $A[V_2]O_4$ have shown that the passage from the localized to itinerant-electron limit occurs through an intermediate phase, in which the Bloch law (i.e., pressure-independent U) breaks down due to the electronic delocalization in cation clusters. $Zn[V_2]O_4$ and $Mg[V_2]O_4$, with small $R_{\text{v-v}}$ may be situated in this intermediate phase [7]. Further, the theoretical calculations show that in $Zn[V_2]O_4$ the electron delocalization leads to a structural instability to form V-V dimers [8], and in $Mg[V_2]O_4$, 6.5 GPa pressure should lead to a metallic conductivity due to the proximity of $R_{\text{v-v}}$ to R_c [7].

However, until now, no direct evidence has been reported to confirm the existence of R_c; for instance, the pressure-induced metallic behavior of the semiconductor $A[V_2]O_4$. Previous pressure studies on resistivity of polycrystalline CoV_2O_4, which is believed to have the smallest V-V separation, actually showed that the activation energy increases with increasing pressure [9]. These results certainly contradict the existence of the critical R_c. Another unsolved issue about CoV_2O_4 is whether it is a normal spinel due to the difficulty of making a stoichiometric sample [10].

In this Letter, we report the structure, magnetization, and resistivity under pressure of $Co[V_2]O_4$ single crystals. The results show that the as-prepared stoichiometric crystal is in close proximity to the itinerant-electron limit on the localized electron side. The comparison between $Co[V_2]O_4$ and other $A[V_2]O_4$ spinels are also made to show the existence of a critical V-V separation.

A single crystal of CoV_2O_4 was grown by the traveling-solvent floating-zone technique. Single crystal x-ray diffraction (XRD) data were collected with a Mo $K\alpha$ source at room temperature. The possible site mixtures between Co and V sites have been tested during the data refinement. The best refinement shows a full occupancy of Co on the A site and V on the B site for the normal spinel $A[B_2]O_4$, which means the site mixture is down to a few percent. The crystallographic data are listed in Table I. The refinement (using FULLPROF with $R_p \approx 7.5$, $R_{\text{wp}} \approx 8.0$, and $\chi^2 \approx 1.3$) of the room temperature powder XRD data obtained on ground crystals with Cu $K_{\alpha 1}$ radiation (1.540 59 Å) [Fig. 1(a)] also confirms the normal spinel structure of the sample. The aligned Laue back diffraction picture along the [100] axis [Fig. 1(b)] further proves the crystal quality. The temperature dependence of the lattice parameter a [Fig. 1(b)] shows a continuous decrease with decreasing temperature and no sign of a structural distortion for $Co[V_2]O_4$ down to 10 K. The thermogravimetric analysis of the sample confirmed the oxygen stoichiometry of 3.99(1).

The temperature dependence of the dc magnetic susceptibility measured with $H = 100$ Oe for $Co[V_2]O_4$ shows a sharp increase around 150 K. At the same temperature, the specific heat shows a peak [Fig. 2(a)]. This magnetic

TABLE I. Room temperature crystallographic data for $Co[V_2]O_4$. (a) $R_1 = \sum || F_o | - | F_c || / \sum | F_o |$, (b) $wR_2 = [\sum w(F_o{}^2 - F_c{}^2)^2 / \sum w(F_o{}^2)^2]^{1/2}$, $w = [\sigma^2(F_o)^2 + (A \cdot p)^2 + B \cdot p]^{-1}$, and $p = (F_o{}^2 + 2F_c^2)/3$; $A = 0.0067$, $B = 0$.

Space Group	$Fd\bar{3}m$ (No. 227)
a (Å)	8.4073(1)
Z	8
Atom Positions, $U_{\rm iso}$	Co 0.375, 0.006 70(13)
$(x = y = z)$	V 0, 0.005 68(12)
	O 0.239 79(10), 0.0071(2)
V (Å^3)	594.251(12)
$\rho_{\rm cal}$ (g/cm^3)	5.026
μ (mm^{-1})	11.497
Data Collection Range (deg)	$8.06 < \theta < 61.47$
Reflections Collected	7124
Independent Reflections	$260[R_{\rm int} = 0.097]$
Parameter Refined	8
R_1, wR_2 $(F_o > 4\sigma F_o)$	0.0370, 0.1035
R_1, wR_2 (All Data)	0.0398, 0.1015
Goodness-of-Fit	1.112

transition is most likely a ferrimagnetic ordering similar to that of $Fe[V_2]O_4$ ($T_C = 106$ K) [11] and $Mn[V_2]O_4$ ($T_C = 56$ K) [12] where the Co (Fe, Mn) spins and V spins align to the opposite direction. The susceptibility shows a cusp around 75 K with irreversibility of zero field cooling and field cooling data below it, which is related to the movement of magnetic domains. Similar results have been reported for other ferrimagnetic spinels [13].

The analysis of the spontaneous magnetization M_s and the initial susceptibility χ_0 is performed based on the M-H curve measurements. In the region around the magnetic phase transition, $M_s \sim t^{\beta}$ for $T < T_C$ and $\chi_0 \sim t^{-\gamma}$ for $T > T_C$ with $t = | T - T_C | / T_C$ [14]. The modified Arrott plot technique [15] was used to determine T_C, β, and γ for M_s and $1/\chi_0$. M_s as a function of the temperature is determined from the intersection of the linear extrapolation of the straight line in the modified Arrott plots with the $M^{1/\beta}$ axis, while $1/\chi_0$ corresponds to the intersection of these lines with the $(H/M)^{1/\gamma}$ axis. Figure 2(c) shows the optimum fitting for $Co[V_2]O_4$ with $\beta = 0.24$, $\gamma = 1.80$, and $T_C = 151.8$ K. For comparison, the same analysis is performed for a $Fe[V_2]O_4$ single crystal [Fig. 2(d)], which gives $\beta = 0.38$, $\gamma = 1.38$, and $T_C = 106.5$ K. The normalized isotherms of the fitting, $t^{-(\gamma+\beta)}H \sim Mt^{-\beta}$ curves (not shown here), show that all of the data points fall on two curves, one for $T < T_C$ and the other one for $T > T_C$, which confirms the validity of the critical exponents.

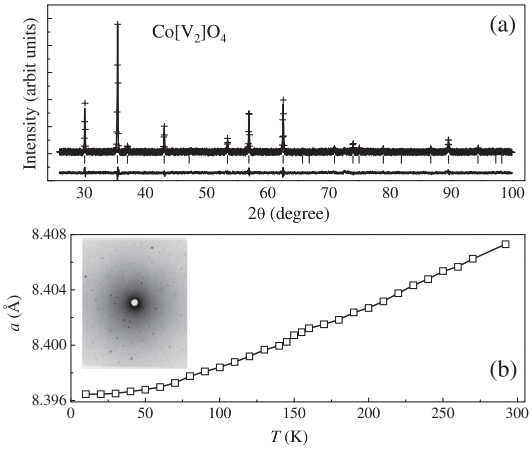

FIG. 1. (a) XRD pattern (crosses) for $Co[V_2]O_4$ at room temperature. (b) Temperature dependence of the lattice parameter for $Co[V_2]O_4$. Insert: Laue back diffraction pattern along the [100] axis.

The temperature dependence of resistivity under different pressures for $Co[V_2]O_4$ is shown in Fig. 3(a). The resistivity was measured with a four probe technique and the pressure was applied on the samples by using a cubic anvil cell. Under ambient pressure, the resistivity shows semiconducting behavior with a lambda-type anomaly around T_C. This behavior is similar to that of the ferrimagnetic chalcogenide spinel, $FeCr_2S_4$ [16], in which the anomaly is attributed to the formation of magnetic polarons [17,18]. Accordingly, the resistivity of $Co[V_2]O_4$ above T_C can be well fitted by $\rho = \rho_0 T \exp(E_P/k_B T)$ for nearest-neighbor hopping of polarons [Fig. 3(c)]. With increasing pressure, the resistivity and E_P both decrease and T_C increases [Fig. 4(a)] at a rate of $d\ln T_C/dP = 3.54 \times 10^{-3}$ kbar^{-1}. T_C is determined as the dip position of $d\ln\rho/dT^{-1}$ vs T curves [Fig. 3(b)]. For $P \geq 6$ GPa, the resistivity shows metallic behavior in the range $115\ {\rm K} < T < T_C$. Our measurements of an as-prepared polycrystalline CoV_2O_4 shows that both resistivity and

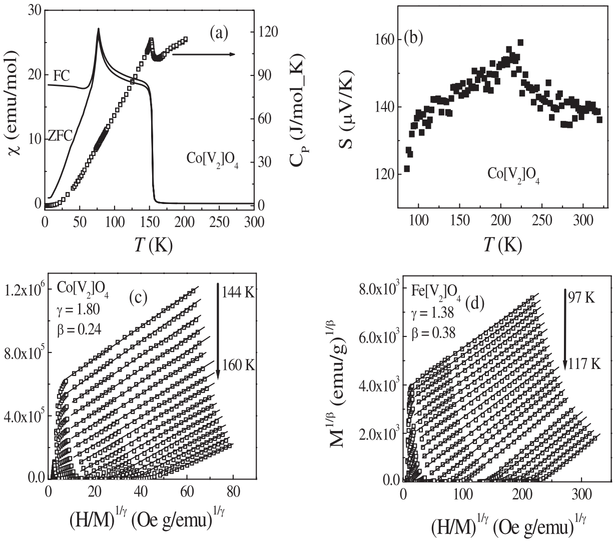

FIG. 2. The temperature dependencies of the susceptibility and specific heat (a) and thermoelectric power (b) for $Co[V_2]O_4$. The modified Arrott plot $M(H)$ for (c) $Co[V_2]O_4$ and (d) $Fe[V_2]O_4$.

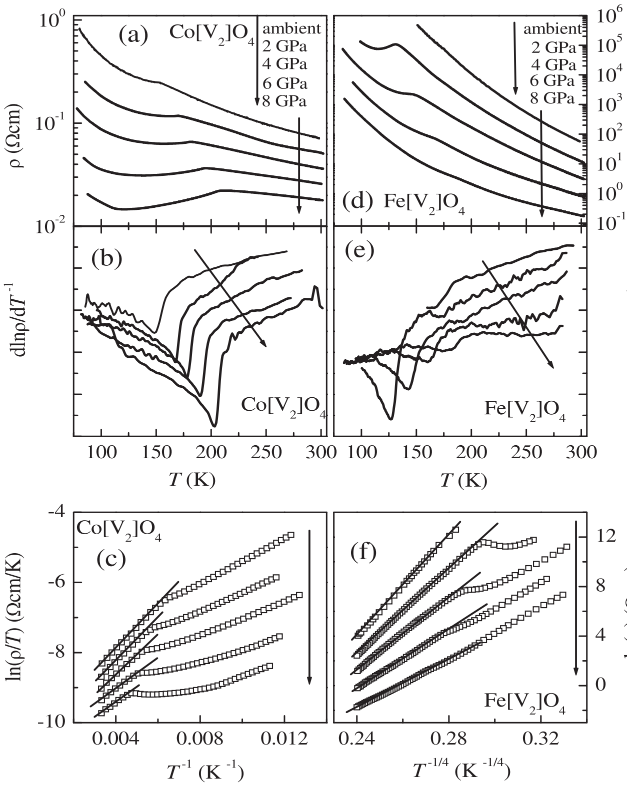

FIG. 3. The temperature dependencies of resistivity (a), $d\ln\rho/dT^{-1} \sim T$ (b), and $\ln(\rho/T) \sim T^{-1}$ (c), measured under different pressures for $\mathrm{Co[V_2]O_4}$. The temperature dependencies of resistivity (d), $d\ln(\rho)/dT^{-1} \sim T$ (e), and $\ln(\rho) \sim T^{-1/4}$ (f), measured under different pressures for $\mathrm{Fe[V_2]O_4}$. In (c) and (f), the solid lines are the fittings as described in the text.

activation energy decrease with increasing pressure, but no metallic conductivity induced up to 8 GPa. For $\mathrm{Fe[V_2]O_4}$ single crystals, with increasing pressure the resistivity decreases and T_C increases at a rate of $d\ln T_C/dP = 6.36 \times 10^{-3}\ \mathrm{kbar}^{-1}$. There is no metallic conductivity induced up to 8 GPa. A better fit for $\mathrm{Fe[V_2]O_4}$ resistivity is achieved with $\rho \propto \exp[(T_0/T)1/4]$, the Mott variable-range hopping (VRH) model [19]. With increasing pressure, T_0 decreases [Fig. 4(a)].

Studies on semiconductor $A\mathrm{[V_2]O_4}$ have pointed out that with decreasing V-V separation, $A\mathrm{[V_2]O_4}$ approaches the itinerant-electron limit. In this limit, $A\mathrm{[V_2]O_4}$ shows abnormal properties. For example, $\mathrm{Mn[V_2]O_4}$ shows a large pressure dependence of T_C with $d\ln T_C/dP = 5.63 \times 10^{-3}\ \mathrm{kbar}^{-1}$, which leads to $\alpha_B = 4.1$, showing the breakdown of the Bloch law [8]. $\mathrm{Fe[V_2]O_4}$ with smaller $R_{\text{v-v}}$ shows a larger $d\ln T_C/dP = 6.36 \times 10^{-3}\ \mathrm{kbar}^{-1}$. Assuming the same compressibility between $\mathrm{Mn[V_2]O_4}$ and $\mathrm{Fe[V_2]O_4}$, for $\mathrm{Fe[V_2]O_4}$ $\alpha_B = 4.6$. This indicates $\mathrm{Fe[V_2]O_4}$ is nearer to the itinerant-electron limit than $\mathrm{Mn[V_2]O_4}$. The large α_B is due to an anomalous compressibility near T_C as predicted for a double-well potential at the crossover from a longer to a shorter equilibrium V-V bond. This double-well potential can perturb the periodic potential to trap the charge carriers, which gives a dominant VRH transport behavior. For VRH model, $T_0 \propto \alpha^3/[k_B N(E_F)]$, where α^{-1} is the localization length, k_B is the Boltzmann constant, and $N(E_F)$ is the density of localized states at Fermi level. It is unlikely that the change of $N(E_F)$ with applied pressure can account for the large decrease of T_0 for $\mathrm{Fe[V_2]O_4}$. Rather, the decrease of T_0 implies the increase of localization length α^{-1}, leading to electronic delocalization.

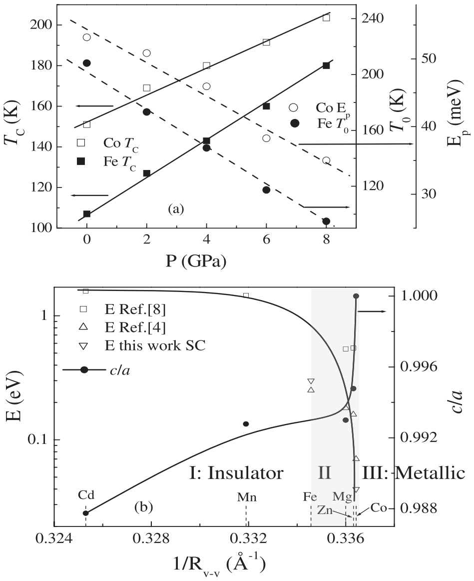

FIG. 4. (a) The pressure dependencies of T_C, T_0, and E_P for $\mathrm{Co[V_2]O_4}$ and $\mathrm{Fe[V_2]O_4}$. (b) E and c/a ratio of $A\mathrm{[V_2]O_4}$ spinels as a function of V-V distance. The solid lines and dashes are just guides to the eye.

$\mathrm{Co[V_2]O_4}$ with $a = 8.4073(1)$ Å at room temperature has the smallest $R_{\text{v-v}} = 2.9724$ Å for semiconducting $A\mathrm{[V_2]O_4}$, which should be even nearer to the itinerant-electron limit than $\mathrm{Fe[V_2]O_4}$. From Fig. 4(b) we can see the activation energy (E) is very large for $\mathrm{Cd[V_2]O_4}$ and $\mathrm{Mn[V_2]O_4}$(∼1 eV) [7], but drops abruptly for Mg, Zn, and Co samples. Under ambient pressure, the Arrhenius fit gives activation energy $E = 300$ and 40 meV above T_C for Fe and Co samples, respectively. The metallic conductivity induced by pressure clearly shows that $\mathrm{Co[V_2]O_4}$ is truly in the itinerant-electron limit. In this limit, the charge carriers will occupy cation clusters as polarons due to the bond disproportionation into molecular orbitals [20], which also means the itinerant-electron clusters are in a matrix of strongly correlated electrons. The nearly temperature-independent thermoelectrical power with a small value 140 μV/K [Fig. 2(b)] and the linear $\ln(\rho/T) \sim T^{-1}$ behavior give strong evidence for the existence of polarons. For $\mathrm{Co[V_2]O_4}$, at higher pressure and lower temperature, the itinerant-electron clusters apparently grow to beyond percolation threshold to induce an overlap of the valence and conduction band, which gives metallic conductivity below T_C when $R_{\text{v-v}}$ passes a critical value. But the strongly correlated volume fraction also percolates to retain the long range magnetic order and lead to the semiconducting behavior below 115 K under high pressure. The *ab initio* calculations on Mg[V_2]O_4 predict a metallic conductivity for $R_c = 2.94$ Å at about 6.5 GPa [7]. Here the metallic conductivity for Co[V_2]O_4 occurs around 6 GPa, consistent with the calculation, assuming a similar compressibility for Mg[V_2]O_4 and Co[V_2]O_4.

Two additional features are noteworthy for Co[V_2]O_4: (i) the abnormal critical exponents and (ii) there is no observable structural distortion from XRD measurements, which means either no or very small structural distortion with $c/a \approx 1$. Further neutron or synchrotron XRD should be performed to determine whether or not there is a weak structural distortion. For Fe[V_2]O_4, $\beta = 0.38$, $\gamma = 1.38$, and $\delta = 4.63$ (calculated from the Widom scaling relation $\delta = 1 + \gamma/\beta$) the exponents are close to the 3D Heisenberg model for a magnetic insulator [21]. However for Co[V_2]O_4, $\beta = 0.24$, $\gamma = 1.80$, and $\delta = 8.5$ do not completely agree with the conventional Heisenberg model. $\gamma = 1.80$ is close to that expected for the magnetic system with a strong disorder when approaching the percolation limit [22]. This disorder may be related to the electronic inhomogeneity in Co[V_2]O_4. For example, for the ferromagnetic transition around a metal-insulator transition with similar electronic inhomogeneity in $La_{0.7}Sr_{0.3}MnO_3$, its critical exponents also deviate from the conventional Heisenberg model [23]. For insulating A[V_2]O_4, where A = Cd or Mn, the orbital ordering of the V^{3+} t_{2g} orbitals leads to a cubic-to-tetragonal structural phase transition with $c/a < 1$. For Cd[V_2]O_4, $c/a = 0.9877$ [24] and for Mn[V_2]O_4, $c/a = 0.9928$ [25], as shown in Fig. 4(b). With decreasing $R_{\text{V-V}}$ or as the system approaches the itinerant-electron limit, c/a increases sharply for Mg [26] and Zn samples [27], which means the magnitude of the structural distortion decreases. For Zn[V_2]O_4, $c/a = 0.9949$ [27]. Here the Fe compound is not considered because the Fe-tetrahedral distortion gives a tetrahedral phase with $c/a > 1$ [11]. The electronic structure calculation for Zn[V_2]O_4 [8] actually shows its structural instability (the formation of homopolar V-V valent bonds) is due to its partial electronic delocalization instead of orbital ordering as in Cd and Mn compounds. The stronger electronic delocalization for Co[V_2]O_4 can lead to more dynamic homopolar V-V covalent bonds with fluctuating long and short V-V bonds, which involves no obvious structural distortion with $c/a \approx 1$.

Previous pressure studies on polycrystalline sample Co[V_2]O_4 gave opposite observations: with increasing pressure the activation energy increased [9]. This result has been explained as the result of the cation deficiency in an unstoichiometric sample [4,28]. A further conclusion was that the changes of V-V separation induced by either temperature or pressure had surprisingly little effect on the localized-itinerant electronic transition, and R_c was only relevant at room temperature and ambient pressure [4]. Our pressure studies on single crystals Fe[V_2]O_4 and Co[V_2]O_4 clearly demonstrate that pressure and temperature do indeed effect the electronic properties strongly by changing the V-V separation. For Fe[V_2]O_4, pressure partially delocalizes the charge carriers. For Co[V_2]O_4 which sits on the edge of the itinerant-electron limit, pressure actually induces metallic conductivity, and shows that R_c is applicable in A[V_2]O_4.

This work is supported by NSF-DMR-0654118 and the State of Florida. A. Kismarahardja is supported by NSF-DMR 0602859 and the work in ISSP is supported by Grant-in-Aid for Research (No. 21340092, No. 20102007, and No. 19GS0205) from the Ministry of Education, Culture, Sports, Science and Technology, Japan. H. D. Z. thanks J. G. Cheng for his help on thermoelectrical power measurement.

---

*zhou@magnet.fsu.edu

[1] S. H. Lee *et al.*, J. Phys. Soc. Jpn. **79**, 011004 (2010).
[2] D. B. Rogers *et al.*, J. Phys. Chem. Solids **24**, 347 (1963).
[3] D. B. Rogers *et al.*, J. Appl. Phys. **35**, 1069 (1964).
[4] J. B. Goodenough, in *Metallic Oxides*, edited by H. Reiss, Progress in Solid State Chemistry (Pergamon, New York, 1972), Vol. 5.
[5] P. W. Anderson, Phys. Rev. **115**, 2 (1959).
[6] D. Bloch *et al.*, J. Phys. Chem. Solids **27**, 881 (1966).
[7] S. Blanco-Canosa *et al.*, Phys. Rev. Lett. **99**, 187201 (2007).
[8] V. Pardo *et al.*, Phys. Rev. Lett. **101**, 256403 (2008).
[9] A. Sawaoka *et al.*, Solid State Commun. **3**, 155 (1965).
[10] D. B. Rogers *et al.*, J. Phys. Chem. Solids **27**, 1445 (1966).
[11] T. Katsufuji *et al.*, J. Phys. Soc. Jpn. **77**, 053708 (2008).
[12] S. H. Baek *et al.*, Phys. Rev. B **80**, 140406(R) (2009).
[13] Z. R. Yang *et al.*, Appl. Phys. Lett. **79**, 3645 (2001).
[14] H. Eugene Stanley, *Introduction to Phase Transitions and Critical Phenomena* (Oxford University Press, New York, 1971), p. 39.
[15] A. Arrott *et al.*, Phys. Rev. Lett. **19**, 786 (1967).
[16] A. P. Ramirez *et al.*, Nature (London) **386**, 156 (1997).
[17] Z. Yang, S. Tan, and Y. Zhang, Phys. Rev. B **64**, 024401 (2001).
[18] Z. Yang *et al.*, Phys. Rev. B **69**, 144407 (2004).
[19] N. F. Mott and E. A. Davis *Electronic Processes in Noncrystalline Materials* (Clarendon, Oxford, 1979).
[20] J. B. Goodenough, Prog. Solid State Chem. **5**, 145 (1971).
[21] M. Seeger *et al.*, Phys. Rev. B **51**, 12585 (1995).
[22] M. E. Fisher, Phys. Rev. **176**, 257 (1968).
[23] K. Ghosh *et al.*, Phys. Rev. Lett. **81**, 4740 (1998).
[24] M. Onoda and J. Hasegawa, J. Phys. Condens. Matter **15**, L95 (2003).
[25] K. Adachi *et al.*, Phys. Rev. Lett. **95**, 197202 (2005).
[26] H. Mamiya *et al.*, J. Appl. Phys. **81**, 5289 (1997).
[27] M. Reehuis *et al.*, Eur. Phys. J. B **35**, 311 (2003).
[28] D. B. Rogers *et al.*, J. Phys. Chem. Solids **27**, 1445 (1966).